162 Aberrations, optical models
Sunday, May 07, 2017 3:15 PM–5:00 PM
Exhibit/Poster Hall Poster Session
Program #/Board # Range: 1117–1141/B0537–B0561
Organizing Section: Visual Psychophysics/Physiological Optics

Program Number: 1117 **Poster Board Number:** B0537
Presentation Time: 3:15 PM–5:00 PM
Corneal shape and optical properties: principal component analysis of corneal Zernike coefficients and comparison with other wavefront error representations
Jens Buehren[1, 2], Mehdi Shajari[2], Krishna Pojita Vunnava[2], Thomas Kohnen[2]. [1]Augenpraxisklinik Triangulum, Hanau, Germany; [2]Department of Ophthalmology, Goethe University, Frankfurt am Main, Germany.
Purpose: To describe the corneal wavefront error with principal components obtained fronm corneal Zernike coefficients and to compare the ability of the novel wave error representation with other wavefront error representations.
Methods: From 792 normal eyes of 495 patients, corneal tomography scans were taken with a commercial Scheimpflug system (Pentacam HR, Oculus, Germany). Based on a ray tracing model, total corneal wavefront aberrations were calculated using a Zernike decomposition up to the 6th order over a pupil diameter of 6 mm. From 27 Zernike coefficients, a principal component analysis (PCA) based on the correlation matrix was performed (SPSS 11.0, Varimax rotation). Coefficient loads of less than |0.25| were ignored. For component selection, an eigenvalue of >1 was applied. Wavefront errors were built up in a stepwise fashion using the novel components, of which each contained a subset of Zernike coefficients. Similarly, wavefront errors were described with single Zernike coefficients by the root-mean square (RMS) of Zernike orders 3-6 and by the RMS of all coma, spherical and residual aberrations. For each wavefront error, the optical quality metric BCVSOTF (visual Strehl ratio based on the optical transfer function, simulated for best spectacle correction) was computed (VOL-Pro 7.14, Sarver and Ass.). The number of components to explain 95% of the variance of BCVSOTF was compared.
Results: PCA produced 11 components with an eigenvalue >1, accounting for 72% of the total variance. The first 4 components accounted for 95% of the BCVSOTF variance. Using individual Zernike modes, 9 coefficients were necessary to describe 95% of the BCVSOTF variance. For wavefront description with RMS values three components were needed each to describe at least 95% of BCVSOTF variance.
Conclusions: Novel wavefront components obtained by PCA were able to describe corneal optical properties as comprehensively as coarser representations such as RMS of Zernike orders.
Commercial Relationships: Jens Buehren, Novartis (I), Oculus (C), Carl Zeiss Meditec (I), Johnson & Johnson (I); **Mehdi Shajari**, Oculus (C); **Krishna Pojita Vunnava**, None; **Thomas Kohnen**, Oculus (C), Alcon (C)

Program Number: 1118 **Poster Board Number:** B0538
Presentation Time: 3:15 PM–5:00 PM
ASSESSMENT OF CORNEAL ABERRATIONS SECONDARY TO PTERYGIUM COMPARED WITH NON-AFFECTED EYES
Edgar Adrian Gonzalez Mendoza[1], Arturo J. Ramirez-Miranda[1], Karla Zuñiga[2], Omar Santana-Cruz[1], Carlos A. Muller Morales[2], Alejandro Navas[1], Enrique O. Graue-Hernandez[1]. [1]Cornea and Refractive Surgery, Institute of Ophthalmology "Conde de Valenciana", Mexico, Mexico; [2]Institute of Ophthalmology "Conde de Valenciana", Mexico, Mexico.
Purpose: To assess and compare both eyes monochromatic-wave aberrations, of subjects with unilateral primary pterygium.
Methods: A prospective, descriptive case series evaluated patients with unilateral primary pterygium. Thirty patients with unilateral primary pterygium underwent corneal aberration study with the Schwind Sirius. Inclusion criteria were patients with unilateral primary pterygium. Patients with ocular pathologies, previous ocular surgery, abnormal findings not related to the pterygium, any abnormal change in the normal fellow eye were excluded. The Zernike coefficient were determined up to the fifth order, and root mean square (RMS) of sphere, cylinder and high order corneal aberrations. All quantitative variables were compared using a paired t test and a p value of less than 0.05 was considered statistically significant. Two-way analysis of variance was used for comparing between eyes with pterygium and the normal fellow eye, also for comparison between both pterygium groups. All data was processed and analyzed using SPSS version 17 (IBM Corp., NY).
Results: Sixty eyes were included of thirty, 11 men (36.7%) and 18 women (63.3%) with a mean age of 52.2 years ± 11.67 years. The mean cylinder value was -1.3 D in pterygium group and - 0.48 D in non-pterygium group, P <0.05. The mean Kmax 47.30 ± 7.81 D in pterygium group and 44.36 ± 1.29 D in non-pterygium group P<0.05. The major aberrations found in eyes without pterygium was astigmatism mean 4.33 μm, trefoil mean 2.25 μm, cuadrifoil mean 1.28 μm, coma mean 0.96 μm, and in affected eyes astigmatism mean 2.62 μm, and trefoil mean 1.26 μm. When we compared both groups all aberrations was statistically different, least spherical aberration p<0.05; and all the aberrations were bigger in eyes with pterygiums >2mm.
Conclusions: Pterygium leads to deterioration of visual performance by causing a significant increase in corneal aberrations. The size of pterygium is a factor that determines the grade of aberration. This study demonstrated that even incipient pterygium, <2 mm can cause corneal abnormalities. Further studies are necessary to evaluate changes in this other aberrations posterior to surgical treatment.
Commercial Relationships: Edgar Adrian Gonzalez Mendoza; **Arturo J. Ramirez-Miranda**, Carls Zeiss Meditec (C), Laboratoires Théa (C); **Karla Zuñiga**, None; **Omar Santana-Cruz**, None; **Carlos A. Muller Morales**, None; **Alejandro Navas**, Alcon Laboratories, Inc (C); **Enrique O. Graue-Hernandez**, None

Program Number: 1119 **Poster Board Number:** B0539
Presentation Time: 3:15 PM–5:00 PM
Measurement of anterior and posterior artificial cornea curvature for anterior segment optical coherence tomography
Futoshi Taketani[1], Mariko Hasegawa[1], Chika Miyazaki[1], Kaori Morii[2]. [1]Ophthalmology, Hyogo Prefectural Amagasaki General Medical Center, Amagasaki, Japan; [2]Asagiri Hospital, Akashi, Japan.
Purpose: To evaluate accuracy of the anterior segment optical coherence tomography (A-OCT) by measuring artificial corneal shape.

Methods: We made four different types of artificial cornea by polymethylmethacrylate (PMMA).
1. Anterior curvature (R) 7.00mm, Posterior R 6.80mm, Central thickness(CT) 0.50mm
2. Anterior R 7.70, Posterior R 6.80, Central thickness(CT) 0.50
3. Anterior R 8.20, Posterior R 6.80mm, Central thickness(CT) 0.50
4. Anterior R 7.67(aspherical), Posterior Rs: 6.73, 90°, Rf: 6.88, 180°(posterior corneal astigmatism), Central thickness(CT) 0.50
5. Anterior Rs: 7.61, 90°Rf : 7.73, 180°, Posterior Rs: 6.64, 180°, Rf: 7.27, 90°(Anterior and posterior corneal astigmatism was perpendicularly)
6. Anterior Rs: 7.61, 90°Rf : 7.73, 180°, Posterior Rs: 6.64, 90°, Rf: 7.27, 180°(Anterior and posterior corneal astigmatism was parallelly)
(unit is mm)
We measured artificial corneal shape in a fluid-filled model constructed to replicate the optical condition of a pseudophakic human eye [1)] by A-OCT (CASIA, Tomay, Nagoya, Japan)
1. Taketani F, Hara Y. Characteristics of spherical aberrations in 3 aspheric intraocular lens models measured in a model eye. J Cataract Refract Surg. 2011 ;37:931-6
Results: We revealed the measured anterior and posterior corneal curvatures at 3mm diameter as follow:
1. Anterior R 7.02, Posterior R 6.80 2. Anterior R 7.72, Posterior R 6.82
3. Anterior R 8.25, Posterior R 6.84 4. Anterior R 7.70, Posterior Rs 6.73, Rf 6.89
5. Anterior Rs: 7.64, 90°, Rf : 7.76, 180°, Posterior Rs: 6.31, 4°, Rf: 7.22, 94°
6. Anterior Rs: 7.64, 90°, Rf : 7.78, 180°, Posterior Rs: 6.32, 93°, Rf: 7.20, 3°
Conclusions: We could measure anterior and posterior artificial corneal curvature correctly by A-OCT. We would use this A-OCT to evaluate corneal shapes including posterior corneal astigmatism clinically.
Commercial Relationships: Futoshi Taketani; **Mariko Hasegawa**, None; **Chika Miyazaki**, None; **Kaori Morii**, None

Program Number: 1120 **Poster Board Number:** B0540
Presentation Time: 3:15 PM–5:00 PM
Anatomical Correlates of Increasing and Decreasing Keratometric Astigmatism in Astigmatic Native American Children
Joseph M. Miller[1, 2], Erin M. Harvey[1], Michael W. Belin[1]. [1]Ophthal & Vision Science, University of Arizona, Tucson, AZ; [2]College of Optical Sciences, University of Arizona, Tucson, AZ.
Purpose: To assess anatomical differences in eyes of children with decreasing and increasing keratometric astigmatism (DKA, IKA) compared to children with stable keratometric astigmatism (SKA).
Methods: Subjects are Native American children who participated in at least two eye exams. Keratometry and autorefraction (Retinomax K-Plus2, Nikon, Melville NY) were performed at both exams, corneal tomography (Pentacam, Oculus, Wetzlar Germany) was performed at only the second exam. Apical pachymetry and SimK radii of curvature were used to derive radial corneal thickness (RCT) at the 3.5mm pupil margin, and an eye model was developed to derive ELP (SEQ and Cyl). Multinomial logistic regressions on right eye data comparing the DKA and IKA groups to the SKA group were performed within each ocular measure at baseline and final exam, and change from first to final exams.
Results: The sample of 317 children (xx DKA, xx IKA, xx SKA), ranging in age from xx to xx at baseline exam, were followed an average of 8 years. The Table summarizes findings by group, along with significant ($p<0.05$) findings (shaded).
Conclusions: These findings indicate that at the final exam, DKA and IKA exhibit similar corneal thickness rotational symmetry. The steeper and flatter meridian are closely aligned, and meridional differences in thickness are ~6 microns, or ~1% corneal thickness. It does not appear that the lens astigmatism differs between eyes showing DKA and IKA. While groups are similar at the final exam, we lack evidence that they were also similar at the first exam, as we did not have Pentacam data for the first observation. We hypothesize that external forces may remodel a relatively stable cornea over time. These findings suggest that the high prevalence of astigmatism in this population is not associated with the relative corneal thinning of keratoconus.

Description of Variable	Decreasing Keratometric Astigmatism (DKA) n=106		Stable Keratometric Astigmatism (SKA) n=106		Increasing Keratometric Astigmatism (IKA) n=105	
	Mean	SEM	Mean	SEM	Mean	SEM
Stratification						
Change in Rmax Ker Cyl, D	-0.519	0.039	0.19	0.015	0.884	0.042
Interval First to Last Exam, Years	7.76	0.244	8.095	0.262	7.372	0.226
Change in Rmax Ker Cyl, D/Year	-0.072	0.006	0.024	0.002	0.121	0.005
Initial Exam Measures						
Age, Years	4.913	0.129	4.893	0.118	5.18	0.13
Rmax Ant Steeper ROC, mm	7.795	0.026	7.748	0.026	7.73	0.029
Rmax Ant Flatter ROC, mm	8.232	0.028	8.127	0.028	8.106	0.027
Rmax Refraction SEQ, D	0.613	0.131	0.912	0.148	0.893	0.145
Rmax Refraction Cyl, D	1.731	0.121	1.557	0.142	1.579	0.132
Final Exam Measures						
Age, Years	12.672	0.251	12.988	0.269	12.552	0.234
Rmax Ant Steeper ROC, mm	7.862	0.026	7.744	0.026	7.656	0.03
Rmax Ant Flatter ROC, mm	8.200	0.025	8.160	0.028	8.196	0.027
Refraction SEQ, D	-0.59	0.196	-0.265	0.199	-0.579	0.203
Refraction Cyl, D	1.314	0.137	1.702	0.161	2.582	0.173
Pentacam Ant Steeper ROC, mm	7.858	0.026	7.74	0.026	7.663	0.03
Pentacam Ant Flatter ROC, mm	8.227	0.025	8.184	0.027	8.222	0.029
Pentacam Post Steeper ROC, mm	6.322	0.026	6.239	0.027	6.156	0.027
Pentacam Post Flatter ROC, mm	6.847	0.026	6.796	0.026	6.832	0.027
Apical Pachymetry, micron	545.5	2.83	548.8	3.18	550.7	2.93
Final Exam Derived Values						
Change in Rmax Steeper ROC, mm	0.066	0.008	-0.003	0.004	-0.074	0.008
Change in Rmax Flatter ROC, mm	-0.032	0.011	0.033	0.004	0.09	0.007
Change in Refraction SEQ, D	-1.204	0.131	-1.177	0.141	-1.472	0.124
Change in Refraction Cyl, D	-0.417	0.07	0.145	0.048	1.002	0.079
Effective Lens, SEQ D	19.777	0.198	19.020	0.218	19.195	0.231
Effective Lens, Cyl D	0.628	0.031	0.712	0.031	0.784	0.047
Meridional Ant-Post Misalign, Deg	0.761	0.959	-0.297	0.469	-0.186	0.95
Pupil Pach, steeper, micron	574.3	2.87	577.3	3.30	579.9	3.03
Pupil Pach, flatter, micron	567.0	2.83	570.6	3.28	572.3	3.00
Pupil Steeper-Flatter Diff, micron	7.346	0.36	6.662	0.36	7.618	0.43

Shaded cells indicate significantly different from SKA group (Multiple Logistic Regression, $p< 0.05$). SEM=Standard Error of Measurement, Rmax=Retinomax K-Plus2, Ker=Keratometry, SEQ=Spherical Equivalent, Cyl=Cylinder, Ant=Anterior Curvature, Post=Posterior Curvature, ROC=Radius of Curvature, Effective Lens=Effective Lens Power (derived), Deg=Degrees, Pupil Pach=Pachymetry at margin of 3.5mm pupil, Meridional Ant-Post Misalign=Misalignment of Anterior and Posterior Axis, Pupil Steeper-Flatter Diff=Difference in Pachymetry for Steeper and Flatter Meridia at margin of 3.5mm Pupil.

Table of Anatomical Characteristics of children exhibing decreasing or increasing astigmatism over time.
Commercial Relationships: Joseph M. Miller, None; **Erin M. Harvey**, None; **Michael W. Belin**, Oculus (C)
Support: NEI-NIH EY13153 (EMH); RPB (JMM)

Program Number: 1121 **Poster Board Number:** B0541
Presentation Time: 3:15 PM–5:00 PM
Analysing the impact of a misaligned toric intraocular lens on wave front aberrations
Natascha Bayer[1], Nino Hirnschall[2], Lukas Traxler[1], Andreas Drauschke[1], Rainer A. Leitgeb[3], Sverker Norrby[4], Oliver Findl[2]. [1]University of Applied Sciences Technikum Vienna, Vienna, Austria; [2]Vienna Institute for Research in Ocular Surgery (VIROS), A Karl Landsteiner Institute, Hanusch Hospital, Vienna, Austria; [3]Medical University Vienna, Center for Medical Physics and Biomedical Engineering, General Hospital Vienna, Vienna, Austria; [4]Landauerlaan 17, Leek, Netherlands.
Purpose: Misalignments of intraocular lenses (IOLs) after cataract surgery influence the image quality negatively. Parameters to judge the effect of misalignments on visual performance are wave front aberrations. The effect of a decentred and tilted toric IOL on wave front aberrations was tested using numerical raytracing software.

Methods: An astigmatic model eye was implemented using the optical ray tracing program Optic Studio (Zemax). As basis for modelling the Liou & Brennan schematic eye was chosen, having a 5° temporal tilt of the visual axis and a 0.5 mm nasal decentration of the pupil. In order to simulate a pseudophakic eye, the IOL was introduced into the model, so that the first principal plane of the natural lens of the Liou & Brennan eye coincides with the first principal plane of the IOL. This refers to an anterior chamber depth of 5.32 mm. The IOL was further characterized by a toric anterior surface and an aspheric posterior surface. In order to simulate a certain degree of astigmatism the anterior surface of the cornea was adapted to a biconic surface with 49.89D @180° and 46.89D @90°. The thickness of 0.5 mm, the refractive index of 1.376 and the conic constant -0.18 were adopted from the data published by Liou & Brennan. The posterior corneal surface was modelled as conic surface having a radius of curvature of 6.4 mm and a conic constant of -0.6. IOL decentration ranged from -0.5 mm to +0.5 mm along the x-axis, while tilt was performed around the y-axis amounting -5° to +5°. Zernike coefficients up to the 4th order were analysed in dependence on tilt and decentration.
Results: An increase of decentration leads to a reduced performance of the toric IOL. This effect maximizes if both tilt and decentration are prominent. The coefficients, which are influenced the most by an IOL misalignment, are defocus (Z_4), astigmatism (Z_6), and coma (Z_8). Spherical Aberration (Z_{11}) shows more sensitivity to IOL decentration than tilt. Minimal influence is also investigated concerning secondary astigmatism (Z_{12}).
Conclusions: Numerical simulations allow estimating the effect of lens misalignments on wave front aberrations and other optical quality parameters. Similar to monofocal IOLs, position tolerance for toric IOLs also has clinical relevance when judging the postoperative vision of the patient.
Commercial Relationships: Natascha Bayer, None;
Nino Hirnschall, None; **Lukas Traxler**, None; **Andreas Drauschke**, None; **Rainer A. Leitgeb**, None; **Sverker Norrby**, None;
Oliver Findl, None

Program Number: 1122 **Poster Board Number:** B0542
Presentation Time: 3:15 PM–5:00 PM
Normative values of the visual image quality metric VSX as a function of age and pupil size
Gareth D. Hastings, Jason D. Marsack, Raymond A. Applegate.
College of Optometry, University of Houston, Houston, TX.
Purpose: The visual image quality metric Visual Strehl (VSX) combines a comprehensive description of the optics of an eye (wavefront error (WFE)) with an estimate of the neural processing of the visual system, and has been shown predictive of subjective best focus and well correlated with change in visual performance. Given the demonstrated capability of VSX to quantify the visual quality of optical corrections, especially where residual diopters and RMS WFE fail to do so, this study aimed to establish normative values of best-corrected VSX as a function of pupil size and age.
Methods: Previously collected WFE data from the Texas Investigation of Normal and Cataract Optics (TINCO) study, recorded on one dilated eye of 146 subjects from 20 to 80 years of age, were fit with tenth-order Zernike expansions and scaled to 7, 6, 5, 4, and 3 mm diameters. A set of 95454 sphere, cylinder, and axis combinations were searched for the prescription (termed *best-corrected*) that provided best visual image quality for each eye at each fixed pupil size. Because physiological pupil size decreases with natural aging, VSX was also calculated for physiological pupil sizes under a range of luminances (10^{-4} to 10^4 cd/m^2) as a function of age. Towards validation of the presented norms, VSX was calculated for an independently collected WFE dataset and compared with the confidence intervals (CI) of the corresponding norms.
Results: Best corrected VSX as a function of age and pupil size quantitatively agreed with the prevailing qualitative understanding of image quality, that is, best visual image quality was found in young eyes (20 to 30 years old) at small pupil diameters (3 mm), and VSX decreased as age increased and as pupil size increased, with pupil size causing a more rapid decrease. Both variables had statistically significant influence ($p<0.0001$); multiple regression is logVSX = 0.414 – 0.005*age – 0.122*pupil size. When natural decrease in pupil size with age was considered, VSX was almost constant across age for most luminances.
Conclusions: The 3-D relation of best-corrected VSX, age, and pupil size is presented and 95% CI norms are provided for age groups between 20 and 80 years and pupil sizes from 3 to 7 mm. These norms can be used to evaluate both traditional and wavefront-guided optical corrections provided by refractive surgery, as well as contact lens and spectacle corrections.
Commercial Relationships: Gareth D. Hastings;
Jason D. Marsack, University of Houston (P);
Raymond A. Applegate, University of Houston (P)
Support: NIH/NEI R01EY008520, NIH/NEI R01EY019105, Navy subcontract: N00259-10-P-1354, NIH/NEI P30 EY, The Borish Endowment

Program Number: 1123 **Poster Board Number:** B0543
Presentation Time: 3:15 PM–5:00 PM
Radial averaging of the optical modulation transfer function and its impact on image quality
Alexander Leube[1], David Kern[2], Arne Ohlendorf[1, 2], Siegfried Wahl[1, 2].
[1]Institute for Ophthalmic Research, University Tuebingen, Tuebingen, Germany; [2]Technology and Innovation, Carl Zeiss Vision International GmbH, Aalen, Germany.
Purpose: The currently used method for radial averaging of the modulation transfer function (MTF) (Thibos, 2004) results in tight fluctuations regarding the outcomes. The purpose of the study was to develop a novel method to average the MTF radially and to evaluate the impact on image quality.
Methods: The MTF was calculated from wavefront aberrations up to the 7th radial order (i.Profiler plus, Carl Zeiss Vision) using a Fourier based approach. Applying a 2-D bi-cubic interpolation algorithm (Matlab 2015b, MathWorks), the MTF was resampled for each radial orientations in 1.0° steps for a step size of spatial frequencies (SF) of 1.0 cpd from 1 cpd up to 60 cpd. Each SF was averaged from 0° to 359° separately, using the same number of given values. To evaluate the impact on image quality of the proposed averaging method, six image quality metrics (IQM) (visible area under the MTF and OTF (AUC), cut-off frequencies for MTF and OTF (SFcutoffMTF, SFcutoffOTF), Square root integral (SQRI) and integrated contrast sensitivity (ICS)) were calculated for natural wavefront errors and artificial combinations of primary coma C(3,-1) and trefoil C(3,-3) from -0.8 μm to +0.8μm.
Results: Bi-cubic pre-sampling of the MTF resulted in a radial averaged MTF (rMTF), representing the mathematically correct mean and results in a smooth outcome without random fluctuations even for asymmetric MTF curves (see Fig. 1). IQMs showed no significant difference for natural wavefront errors ($p_{All}>0.05$, t-test) and high correlations ($r>0.92$, $p<0.001$, Pearson) between the two rMTF methods. For combinations of C(3,-1) and C(3,-3) that differed in the sign, AUC-based metrics result in significantly lower values, when the proposed rMTF method was used ($\Delta AUC_{MTF}=-0.04$, $p=0.04$; $\Delta AUC_{OTF}=-0.05$, $p=0.002$; $\Delta ICS=-95.33$, $p=0.02$; t-test). SFcutoffMTF and SQRI metric performed equally well in both

methods (r>0.90, p<0.05, Pearson; p>0.05, t-test) while artificial wavefront errors were used.
Conclusions: The proposed method of pre-sampling the MTF using bi-cubic interpolation, provides a mathematically correct mean rMTF and offers a better estimation of image quality, using area under the curve based metrics, especially in highly asymmetric wavefronts.

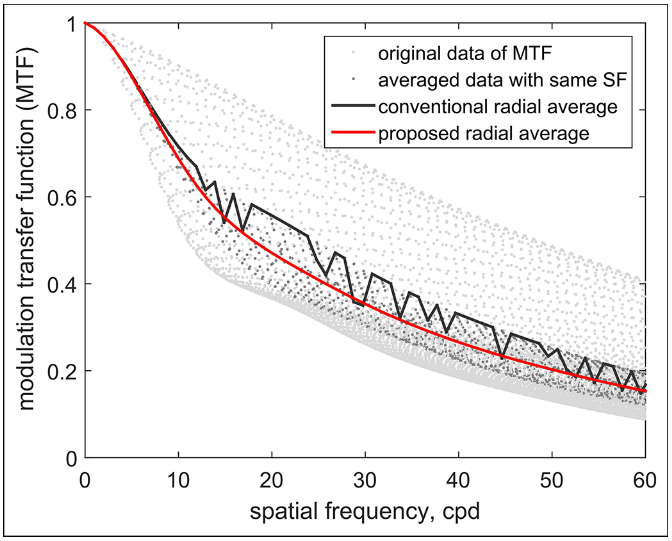

Fig. 1: Example for radial average of modulation transfer function (rMTF) calculated from original data (grey) with the proposed method (red) and the conventional method (black).
Commercial Relationships: Alexander Leube, None; **David Kern**, Carl Zeiss Vision International GmbH (E); **Arne Ohlendorf**, Carl Zeiss Vision International GmbH (E); **Siegfried Wahl**, Carl Zeiss Vision International GmbH (E)

Program Number: 1124 **Poster Board Number:** B0544
Presentation Time: 3:15 PM–5:00 PM
Profile of off-axis higher order aberrations and its variation with time
Krupa Philip[1], Padmaja Sankaridurg[2, 1], Arthur Ho[1, 2], Thomas J. Naduvilath[2], Paul Mitchell[3]. [1]School of Optometry and Vision Science, University of New South Wales, Sydney, NSW, Australia; [2]Brien Holden Vision Institute, University of New South Wales, Sydney, NSW, Australia; [3]Westmead Millenium Institute, University of Sydney, Sydney, NSW, Australia.
Purpose: To quantify the profile of peripheral higher order aberrations (HOA) in eyes of adolescents and to determine change if any in the HOA after 5 years.
Methods: Children (646) were measured as part of the Sydney Myopia Study (age 12.7 ± 0.4 years) and followed-up approximately 5 years later in the Sydney Adolescent Vascular and Eye Study (age, 17.1 ± 0.5 years). Peripheral HOA were measured at 30 degrees temporal (T), nasal (N) and inferior (I) visual field under cycloplegia (5 mm pupil diameter) using COAS aberrometer. One-way ANOVA and paired t-test were done.
Results: At baseline, 176 (27%) eyes were emmetropic (SE +0.15 ± 0.24D), 95 (15%) were myopic (SE -2.00 ± 1.38D) and remaining 375 (58%) were hyperopic (SE +1.09 ± 0.66D). Of the peripheral HOA, C(4,0) was more positive for hyperopic (N:+0.050 ± 0.058μm,I:+0.067 ± 0.061μm,T:+0.057 ± 0.054μm) compared to myopic (N:+0.027 ± 0.056μm,I:+0.052 ± 0.057μm,T:+0.020 ± 0.048μm) and emmetropic eyes (N:+0.022 ± 0.052μm, I:+0.049 ± 0.056 μm, T:+0.026 ± 0.043 μm) ($p < 0.05$).
At follow up, 26 % (n=167) had '*myopic change*' (change in SE≥ -0.50D) and 70% (n=451) had '*no change*' (change in SE= -0.49D to +0.49D). Coma aberrations [C(3,-1) and C(3,1)] at nasal field became more negative for all eyes at follow-up irrespective of '*myopic change*' or '*no change*' (p<0.05). At follow-up, spherical aberration became more positive at temporal field for emmetropic and myopic eyes in '*no change*' group (p<0.05). Also, HOA RMS increased for eyes with '*myopic change'* for myopic (increase at T field by 0.019 ± 0.068 μm, p = 0.011) and hyperopic eyes (increase at T field by 0.024 ± 0.071, p =0.006 and increase at N field by 0.020 ± 0.080 μm, p=0.039) and for emmetropic eyes (increase at T field by 0.025 ± 0.061 μm, p=0.011). In addition, emmetropic eyes with '*no change*' also registered an increase in HOA (increase at T field by 0.021 ± 0.072 μm, p = 0.001 and increased at I field by 0.025 ± 0.103 μm, p=0.006).
Conclusions: With increasing age, spherical aberration became more positive at temporal field for emmetropic and myopic eyes that did not undergo a change in refraction. Coma aberrations became more negative at nasal field irrespective of refractive error change at follow-up. With increasing age, HOA RMS at peripheral visual field especially the temporal field increased and was significant for eyes with myopic change in refraction.
Commercial Relationships: Krupa Philip, None; **Padmaja Sankaridurg**, None; **Arthur Ho**, None; **Thomas J. Naduvilath**, None; **Paul Mitchell**, None
Support: NHMRC (Grant ID 52530)

Program Number: 1125 **Poster Board Number:** B0545
Presentation Time: 3:15 PM–5:00 PM
Scleral radius estimation based on anterior eye surface
Izabela K. Garaszczuk[1, 2], Maryam Mousavi[2], Alejandro Cervino Exposito[1], Dorota H. Szczesna-Iskander[3], Robert Iskander[2], Danilo Andrade de Jesus[2]. [1]Optics, Optometry and Vision Science, University of Valencia, Burjassot, Spain; [2]Biomedical Engineering, Wroclaw University of Science and Technology, Wroclaw, Poland; [3]Optics and Photonics, Wroclaw University of Science and Technology, Wroclaw, Poland.
Purpose: To precisely estimate scleral radius based on spherical approximation using scleral topography.
Methods: Eye Surface Profiler (ESP, Eaglet-Eye, Netherlands) was used to acquire the anterior eye surface. Twenty-three emmetropic subjects aged 28.1 ± 6.6 years (range from 20 to 45) volunteered for the study. For comparison purposes, a low myopic (-2.0 D) and a high myopic (-6.5D) subjects were measured. Scleral radius was obtained based on the approximation of the topographical scleral data to a sphere using least squares fitting. The spherical approximation with and without the axial length as a reference point was compared. Moreover, the influence of the eye palpebral aperture was studied. Lastly, measurements of corneal radius, central corneal thickness, anterior chamber depth and white-to-white corneal diameter were acquired with IOLMaster 700 (Carl Zeiss Meditec AG, Jena, Germany) and compared to the scleral radius.
Results: The spherical approximation has shown to be highly precise for emmetropic eyes, however, its error has revealed to be proportional to the myopic refraction error. The estimated scleral radius for the emmetropic group considering the axial length and a normal palpebral aperture was 11.2 ± 0.3 mm. The obtained values have shown to be highly precise with a coefficient of variation of 0.4%. Results have shown that Scleral radius can be estimated precisely considering only the anterior surface data if full measurement of scleral region, including inferior and superior parts of sclera, is acquired. A statistically significant correlation between

axial length and scleral radius ($R^2 = 0.957$, $p<0.001$) was observed. Moreover, corneal radius ($R^2 = 0.420$, $p<0.001$), anterior chamber depth ($R^2 = 0.141$, $p=0.039$) and white-to-white corneal diameter ($R^2 = 0.146$, $p=0.036$) have also shown statistically significant correlations with the scleral radius. Lastly, no correlation was observed comparing scleral radius to the central corneal thickness ($R^2 = 0.047$, $p=0.161$).
Conclusions: Three-dimensional topographical data of an emmetropic eye acquired with ESP, can be used to calculate the scleral radius with high precision based on a spherical approximation.
Commercial Relationships: Izabela K. Garaszczuk, None; **Maryam Mousavi**, None; **Alejandro Cervino Exposito**, None; **Dorota H. Szczesna-Iskander**, None; **Robert Iskander**, None; **Danilo Andrade de Jesus**, None
Support: Marie Curie ITN grants, EDEN, 642760 and AGEYE, 608049

Program Number: 1126 **Poster Board Number:** B0546
Presentation Time: 3:15 PM–5:00 PM

Optical Bench Simulation for Intraocular Lenses Using Field-Tracing Technology

inseok song[1], Se Jin Oh[2], Min Ho Kang[3], Seok Ho Song[2].
[1]Yeongdeungpo Lee's eye clinic, Seoul, Korea (the Republic of); [2]Department of Physics, Hanyang University College of Natural Science, Seoul, Korea (the Republic of); [3]Department of Ophthalmology, Hanyang University College of Medicine, Seoul, Korea (the Republic of).

Purpose: To evaluate the image quality of intraocular lenses (IOLs) using field-tracing optical simulation and then compare it with the image quality using conventional ray-tracing simulation.
Methods: We simulated aspheric IOLs with a decenter, tilt, and no misalignment using an aspheric corneal eye model with a positive spherical aberration. The retinal image, Strehl ratio, and modulation transfer function (MTF) were compared between the ray-tracing and field-tracing optical simulation and confirmed by the results reported in an *in vitro* experiment using the same eye model.
Results: The retinal image showed interference fringes from target due to diffraction from the object in a field-tracing simulation. When compared with the experimental results, the field tracing represented the experimental results more precisely than ray tracing after passing over 400 µm of the decentration and 4 degrees of the tilt of the IOLs. The MTF values showed similar results for the case of no IOL misalignment in both the field tracing and ray tracing. In the case of the 200-µm decentration or 8-degree tilt of IOL, the field-traced MTF shows lower values than the ray-traced one.
Conclusions: The field-tracing optical bench simulation is a reliable method to evaluate IOL performance. It can provide retinal image quality close to real by taking into account the wave nature of light, interference and diffraction.

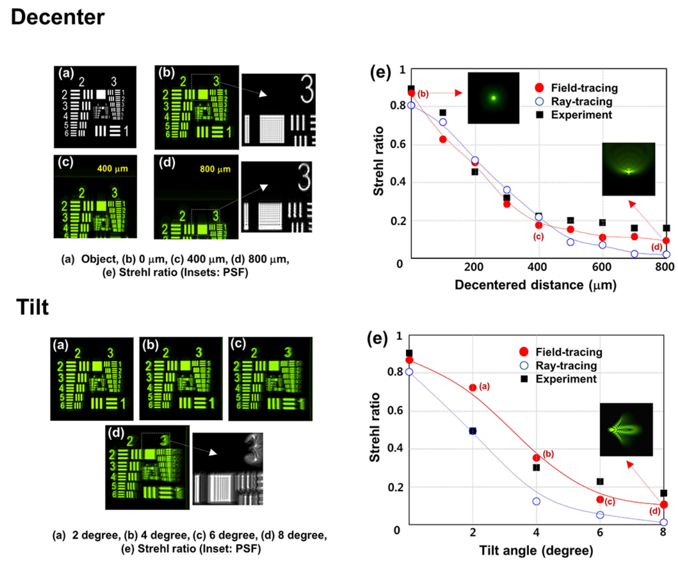

IOL decentration. The 5 mm x 5 mm object (a) is imaged on the screen using field-tracing simulation when the decentered distances of the IOL from the z-axis are 0 µm (b), 400 µm (c), and 800 µm (d). (e) Strehl ratios obtained by field-tracing (filled red circle), ray-tracing (open blue circle), and extraction values (square box) from the reference experiment.
IOL tilt. The images of filed tracing simulation with the tilt angles about the y-axis are 2, 4, 6, and 8 degrees (a,b,c,d). (e) Strehl ratios obtained by field-tracing (filled red circle), ray-tracing (open blue circle), and extraction values (square box) from the reference experiment.

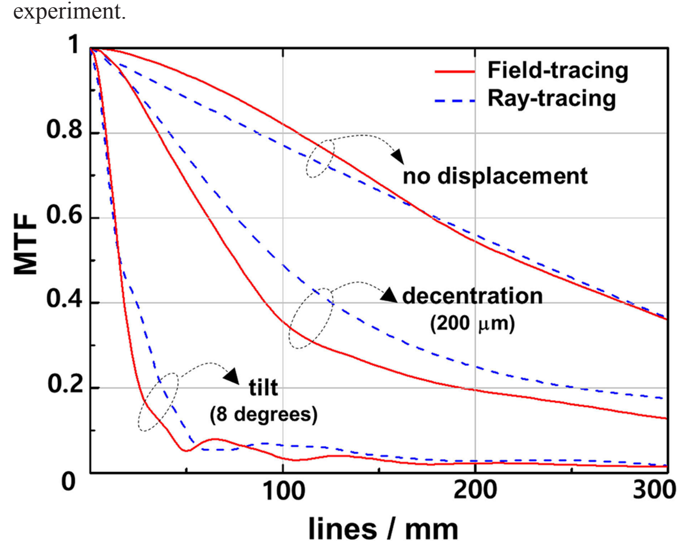

The MTF values of the IOL by field tracing (solid red curve) and ray tracing (dashed blue curve) for the case of no misalignment, 200-µm decentration, and 8-degree tilt. For the case of no misalignment, similar results were obtained for both of the tracing methods but not for the decentration or tilt.
Commercial Relationships: inseok song, None; **Se Jin Oh**, None; **Min Ho Kang**, None; **Seok Ho Song**, None

Program Number: 1127 **Poster Board Number:** B0547
Presentation Time: 3:15 PM–5:00 PM

Evaluation of a Night Spectacle Correction concerning an Improvement of Mesopic Vision Quality

Philipp Hessler, Maria Stinn, Josefine Dolata, Stephan Degle. Ernst-Abbe-University of Applied Sciences Jena, Klingenberg, Germany.

Purpose: Night myopia is discussed to be a possible reason of vision problems in dark light conditions. The aim of this study was to investigate whether quality of vision in twilight or night could be improved by a spectacle correction optimized for mesopic light conditions. Moreover, objective refraction in large pupils measured by aberrometry was compared to subjective mesopic refraction.

Methods: Data of 100 subjects aged from 18 to 40 were analyzed in this prospective, randomized, double-masked, multicentric cross-over study. For aberrometry, devices of the *Visionix* VX 120 family were used. Study participants' subjective refraction was obtained under both, photopic and mesopic light conditions. In the course of this trial, a conventional spectacle correction for photopic light conditions and a sphero-cylindrical optimized mesopic spectacle correction were tested for two weeks each.

Results: Compared to photopic light conditions visual acuity was found to be physiologically reduced in mesopic conditions by 0.2 logMAR units. Subjective spherical equivalent change was -0.30 ± 0.2 D in mesopic light conditions ($p<0.001$). Components of Astigmatism did not significantly change. With the mesopic correction a median visual acuity improvement of 0.1 logMAR units could be achieved ($p<0.001$). Subjective comfort of vision and sharpness could be improved while subjective glare could be reduced by wearing the mesopic correction ($p<0.01$). 75 % of the subjects reported an improved quality of vision at night when wearing the night spectacle correction. However, changes of pupil size-depended objective refraction values were not comparable to changes in luminance-dependent subjective refraction data.

Conclusions: Wearing spectacles fitted with optimized refraction values for mesopic conditions results in an improvement of mesopic vision quality. Particularly for individuals with night vision complaints, a mesopic subjective refraction should be performed within an optometric examination.

Commercial Relationships: Philipp Hessler; **Maria Stinn**, IGA OPTIC eG (R), IGA OPTIC eG (F); **Josefine Dolata**, IGA OPTIC eG (R); **Stephan Degle**, IGA OPTIC eG (R), IGA OPTIC eG (F)
Clinical Trial: NCT02965534

Program Number: 1128 **Poster Board Number:** B0548
Presentation Time: 3:15 PM–5:00 PM

Blue light transmission of commercially available sunglasses

Mitul Mehta[1], Mohamed Mohamed[1, 2], Hosik Hwang[1], James Jester[1]. [1]Gavin Herbert Eye Institute, University of California Irvine, Irvine, CA; [2]Ophthalmology Department, University of Minia, Minia, Egypt.

Purpose: Nonprescription sunglasses are regulated by the Food and Drug Administration (FDA) and required to conform to safety standards. The U.S. standard is American National Standards Institute (ANSI) Z80.3-2015, which requires the lens to have a UVB (280 to 315 nm) transmittance of no more than 1% and a UVA (315 to 380 nm) transmittance of no more than 0.3X visual light transmittance. The possible association of blue light with age-related macular degeneration (AMD) has led to the promotion of so-called blue-blocking lenses. These lenses absorb radiation in the band 400 nm to 500 nm. The purpose of this study is to compare the short wavelength visible light transmittance properties of different commercially available sunglasses.

Methods: Thorlabs compact CCD spectrometer CCS200 was used for measuring transmittance of 6 different sunglasses in ambient sunlight. Each sunglass was given a code number from 1 to 6 (Table 1). The measurements were recorded on November 12 2016 at noon time under a cloudless sky. The location was in Irvine, California (Latitude: 33.6839° N, Longitude: 117.7947° W). Trace recordings were obtained for unfiltered sunlight as a reference, and then for sunlight filtered through each sunglass. Transmittance of each sunglass was calculated as a percentage using Thorlabs OSA software version 2.00 at 380 nm through 490 nm wavelengths with 10 nm intervals.

Results: Short wavelength transmission was variable among different sunglasses. While most blocked more than 80% of all wavelengths less than 490 nm, some transmitted up to 30%. Specifically 2 sunglasses did not meet ANSI requirement of blocking UV light. Polarized sunglasses did better than non-polarized ones in blocking short wavelength light. Sunglass no. 1 is the only sunglass specifically marketed as a blue blocker, and it did better than all the others in blocking short wavelength light (Table 2).

Conclusions: Our results show variability in short wavelength visible light transmission between different commercially available sunglasses. We propose that blue light transmission properties should be included in labelling of sunglasses, especially those used by early AMD patients as a caution against progression to more advanced stages.

	Polarization	Tint
Sunglass 1	Polarized	Brown
Sunglass 2	Polarized	Brown
Sunglass 3	Non-polarized	Gray
Sunglass 4	Non-polarized	Brown
Sunglass 5	Polarized	Gray
Sunglass 6	Non-polarized	Blue

	Wavelength (nm in air)												
	380	390	400	410	420	430	440	450	460	470	480	490	Transmittance (%)
Sunglass 1	0	0	0	0.66%	1.99%	3.13%	3.89%	4.84%	6.36%	7.69%	9.58%	10.91%	
Sunglass 2	0	0	0	3.41%	7.02%	7.59%	7.59%	7.59%	8.73%	9.68%	11%	11.95%	
Sunglass 3	33.59%	32.45%	31.12%	25.81%	21.25%	18.60%	16.89%	14.04%	22.40%	28.73%	29.98%	29.60%	
Sunglass 4	0	7.02%	15.37%	11.95%	5.50%	3.61%	3.61%	1.90%	5.69%	16.89%	23.15%	23.15%	
Sunglass 5	0	0	0	2.85%	6.45%	8.35%	9.87%	11.58%	13.28%	13.28%	14.23%	14.04%	
Sunglass 6	0	0	0	2.28%	6.64%	8.54%	9.30%	10.82%	11.77%	11.77%	12.90%	12.90%	

Commercial Relationships: Mitul Mehta, None; **Mohamed Mohamed**, None; **Hosik Hwang**, None; **James Jester**, None
Support: Unrestricted Grant from Research to Prevent Blindness, Inc.

Program Number: 1129 **Poster Board Number:** B0549
Presentation Time: 3:15 PM–5:00 PM

The impact of soft contact lens dynamic movement, patient ocular spherical aberration distribution and clinical refraction error on lens visual correction performance

Minghan Chen, Ben Wooley. Johnson and Johnson Vision Care, Jacksonville, FL.

Purpose: Spherical aberration (SPHA) presenting in both soft contact lenses and a wearer's eyes affect visual acuity (VA) by blurring retinal images. Ocular SPHA varies across individuals depending

on various factors including accommodation, age, pupil size and spherical refraction. For a contact lens wearer, the two optical systems might not be aligned since the lens moves dynamically on the eye. In addition to the opto-mechanical aspects, in clinical practice, refraction errors also occur. In this study, simulations were conducted to quantitatively investigate these effects.

Methods: Ocular SPHA distribution was obtained based on clinical measurements and a lens was designed with varying SPHA depending on refraction power. Area modulation transfer function (AMTF) based VA (using as the metric) was calculated to quantitatively evaluate the visual correction performance of the lens design. To account for a lens dynamically moving, a 300 µm standard deviation of lens dynamic movement was assumed. A 0.50D standard deviation was employed as the clinical refraction error. Simulations were conducted based on 100 eyes at 3, 4 and 6 mm pupil size and VA at distance, intermediate and near were calculated.

Results: The interaction of SPHA between lens and eye was shown to affect lens visual correction performance significantly in the accommodation process. With a 6-mm pupil size, on average for contact lens with +0.16 D/mm^2 SPHA, from distance vision (infinity distance) to near vision (2.0D), VA improves from -1.7 to -0.6. While for a contact lens with -0.08 D/mm^2 SPHA, the VA does not vary significantly. For a lens with -0.17 D/mm^2 SPHA, from distance to near vision, the VA deteriorates from -1 to -1.4. Simulations also indicate that the biggest VA degradation of 1.4 was observed with a lens with -0.08 D/mm^2 SPHA at distance due to lens movement, refractive error and patient SPHA distribution.

Conclusions: In general, the lens visual correction performance degrades due to lens movement, ocular SPHA distribution, and clinical refractive error. Interactions between the wearer ocular SPHA and the lens SPHA also have a significant impact on lens vision correction performance especially at distance vision for lens with higher positive SPHA, and near vision for lens with stronger negative SPHA.

Commercial Relationships: Minghan Chen, Johnson and Johnson Vision Care (E); **Ben Wooley**, Johnson and Johnson (I), Johnson and Johnson Vision Care (E)

Program Number: 1130 **Poster Board Number:** B0550
Presentation Time: 3:15 PM–5:00 PM

Objective assessments of tear film quality before and after exposure to controlled environmental stress in young and older subjects

Juan Tabernero[1], Joseph Robinson[1], Pablo Artal[2], Shahina Pardhan[1]. [1]Vision and Eye Research Unit, Anglia Ruskin University, Cambridge, United Kingdom; [2]Laboratorio de Optica, Universidad de Murcia, Murcia, Spain.

Purpose: Dry environments, such as those in offices or air craft cabins, can potentially generate ocular discomfort and alter the tear film. We compare various optical and non-optical parameters in young and older subjects after exposure to dry conditions using a controlled environmental chamber (CEC).

Methods: Twenty-four healthy subjects, covering an age range between 18 to 83 years old, were recruited. Subjects watched a movie (for 1.5 hours) in a CEC with a constant temperature (23°) and low humidity (5%). Various parameters were measured before and after the exposure: i) Objective Scatter Index (OSI) of the eye (OQAS, Visiometrics, Spain), ii) Blinking period over a 5 minutes video using customized image processing routines to detect blinks iii) Tear Film Homogeneity (TFH) using a specially built instrument which recorded the corneal reflection of a 300 LEDs-ring at 100 fps for 45 seconds. A metric, based on the cross-correlation function, was used to assess the tear film during inter-blink periods. Subjects also completed a questionnaire (OSDI) to score symptoms related to dryness.

Results: Light scatter did not change in younger subjects (<40 y.) but increased significantly in older subjects (>60 y.) (p=0.013) after exposure to the dry conditions, and that change was linearly correlated with age when all the data were pooled together (R=0.42; p=0.043). Subjective complaints and light scatter did not correlate significantly, although subjects who showed a large increase in light scatter (four were above a change of 0.25 units of OSI) also reported increased dryness. Blinking period decreased significantly after exposure (p=0.002) in both younger and older subjects with older subjects showing a larger mean difference (-1.0±0.8 sec in younger subjects, -2.6±2.8 sec in older subjects). TFH assessed from corneal reflection did not show statistically significant changes in younger and older subjects, but did deteriorate more in those subjects who had symptoms compared to those without symptoms (unpaired t-test p=0.02).

Conclusions: Exposure to dry environment alters the dynamics of blinking and light scatter, particularly in older subjects. Also, Tear Film Homogeneity showing significant associations with symptoms has a potential for predicting patients who report dry eye symptoms.

Commercial Relationships: Juan Tabernero, None; **Joseph Robinson**, None; **Pablo Artal**, None; **Shahina Pardhan**, None

Program Number: 1131 **Poster Board Number:** B0551
Presentation Time: 3:15 PM–5:00 PM

The influence of age, ethnicity, eye/body size and diet on corneal biomechanics

Janis B. Orr, Madara Zvirgzdina, James Wolffsohn. Life and Health Sciences (Optometry), Aston University, Birmingham, United Kingdom.

Purpose: Orthokeratology (ortho-k) is a convenient, effective method of refractive error correction, and has been shown to play an important role in myopia control. However, there is substantial inter-patient variation in treatment response, which has been attributed to corneal biomechanical factors. Evaluation of the influence of age, ethnicity, eye size (axial length), body size (height/weight) and diet on corneal biomechanics may allow prediction of treatment outcome and aid patient selection.

Methods: One hundred and fifty-eight healthy volunteers were recruited (mean±SD age: 32.4±12.3 years, range 19 to 63 years; mean±SD; mean spherical equivalent, MSE: -1.46±2.25 D, range -11.81 to 3.60 D). Axial length was measured using and an optical biometer (IOL Master 500). Height and weight measurements were taken using a stadiometer and a mechanical scale. Food consumption data were recorded, using an adapted 90 item Food Frequency Questionnaire (FFQ). Corneal biomechanics were measured using the Ocular Response Analyser.

Results: Corneal hysteresis (CH) and corneal resistance factor (CRF) were not influenced by age (CH: p=0.586; CRF: p=0.173), ethnicity (CH: p=0.586; CRF: p=0.493), diet (CH: p=0.681; CRF: p=0.952), height/weight (CH: p=0.35; CRF: p=0.394) or axial length (CH: p=0.256; CRF: p=0.866). However, other ORA derived metrics were significantly influenced by axial length, height/weight, and higher meat intake (all p<0.005).

Conclusions: Whereas ethnicity and age have no influence corneal biomechanics, axial length, height/weight and higher meat intake do influence a number of ORA-derived corneal biomechanical metrics; but not CH or CRF. Variations in the additional ORA-derived parameters reflect the complex nature of corneal biomechanical response, and suggest that they should be considered alongside CH

and CRF, when investigating/predicting corneal biomechanical response to orthokeratology.
Commercial Relationships: Janis B. Orr, None; **Madara Zvirgzdina**, None; **James Wolffsohn**, None
Support: The College of Optometrists Research Fellowship Award

Program Number: 1132 **Poster Board Number:** B0552
Presentation Time: 3:15 PM–5:00 PM
Analysis of newborn ocular biometry as a pre-emmetropization reference
Jos Rozema[1, 2], Zvi Herscovici[3, 4], Ruth Axer-Siegel[3, 4].
[1]Ophthalmology, Universitair Ziekenhuis Antwerpen, Edegem, Belgium; [2]Medicine and Health Science, University of Antwerp, Antwerp, Belgium; [3]Ophthalmology, Rabin Medical Center, Petah Tiqva, Israel; [4]Sackler School of Medicine, Tel Aviv University, Tel Aviv, Israel.
Purpose: During emmetropization the refractive components of the eye change shape and position over a period of several years in order to optimize ocular refraction towards a value of about *+1D*. This work reports the ocular biometry in a group of newborn infants aged *1 – 7* days, before emmetropization has taken place, derived from a number of sources in the literature.
Methods: The newborn biometry was obtained from several sources (Gernet 1964, Luyckx 1966, Insler 1987, Blomdahl 1979, Axer-Siegel 2007), leading to a combined set of *302* eyes. All infants were reported as full-term with gestational ages between *36* and *42* weeks, and measured within *7* days after birth. All sources reported using ultrasound biometry (for axial length L, total anterior chamber depth *ACD* and lens thickness *LT*), keratometry (anterior corneal curvature R_{ca}) and hand-held retinoscopy after cycloplegia (refraction *SE*). From these data the lens power P_L and curvature was estimated using the Bennett and Royston equations, respectively. Full records were available for *59/302* eyes, all others had partial records.
Results: The mean biometry values were $SE = 2.55 \pm 1.39\ D$, $R_{ca} = 7.07 \pm 0.38\ mm$, $ACD = 2.30 \pm 0.15\ mm$, $L = 17.15 \pm 0.67\ mm$, and $P_L = 49.91 \pm 3.29\ D$. The axial length L at birth was significantly correlated with birth weight (Spearman $r = 0.443$, $p < 0.001$), *SE* ($r = -0.298$, $p < 0.001$), R_{ca} ($r = -0.505$, $p < 0.001$), *ACD* ($r = 0.595$, $p < 0.001$) and P_L ($r = -0.664$, $p < 0.001$). Corneal curvature R_{ca} was significantly correlated with birth length ($r = 0.470$, $p < 0.001$) and birth weight ($r = 0.532$, $p < 0.001$). Gestational age was significantly correlated with L ($r = 0.362$, $p = 0.003$) and *ACD* ($r = 0.425$, $p < 0.001$).
Conclusions: These observations are consistent with the notion that at birth most ocular parameters are scalable with respect to axial length, which in turn is associated with gestational age. The values presented may be used as a pre-emmetropization reference for future studies and could be used to develop a newborn eye model.
Commercial Relationships: Jos Rozema; **Zvi Herscovici**, None; **Ruth Axer-Siegel**, None

Program Number: 1133 **Poster Board Number:** B0553
Presentation Time: 3:15 PM–5:00 PM
Measurement of 360° Peripheral Refraction Profile in Emmetropic and Myopic Young Human Eyes
Keyur Savla, Viswanathan Ramasubramanian. Lotus College of Optometry, Mumbai, India.
Purpose: Prior studies have measured refraction along the horizontal, vertical and few oblique retinal eccentricities. However, 360° peripheral refraction profiles of human eyes have not been measured. Hence, the goal of this study was to measure and compare the 360° peripheral refraction profile in emmetropic and myopic eyes.
Methods: Twenty healthy young subjects (10 emmetropes and 10 myopes) aged between 17 to 25 years were recruited. Myopic eyes had spherical refraction of ≤ -3 D and astigmatism of ≤ 2 D. Right eyes were cyclopleged with 1% cyclopentolate eye drops. Three refraction measurements in the right eye were recorded using a Grand Seiko autorefractor (WAM 5500) at each of the predetermined 185 locations across all meridians in 10° steps, spanning a total of 30° horizontal and 15° vertical visual fields. Mean values of spherical equivalent refraction (SER), J_0 and J_{45} were measured at each eccentricity. Sector-wise comparisons were performed along 4 sectors: a) horizontal (nasal-temporal) b) vertical (superior-inferior) c) oblique (superior-temporal inferior-nasal [ST-IN]) and d) superior-nasal inferior-temporal [SN-IT] for both the groups.
Results: In all 4 sectors, the SER for myopic eyes showed a relative hyperopic shift in the periphery, with the temporal periphery becoming almost equal to the foveal refraction at 30° eccentricity. The J_0 component showed relative hyperopia in the nasal half of the retina for the first 15° and then progresses to become more myopic in the periphery for both the emmetropic and myopic subjects. The J_{45} component has a relatively similar outcome for both groups with the ST-IN sector being hyperopic in the periphery and the SN-IT sector being myopic in the periphery. The vertical and horizontal sectors remain relatively close to the foveal refractive error throughout the eccentricities for both the groups.
Conclusions: The study showed that there are significant sector-wise changes in refraction at the periphery as compared to fovea. With all the 360° meridians considered in this study, it provides a valuable insight into an eye's complete refractive error profile.

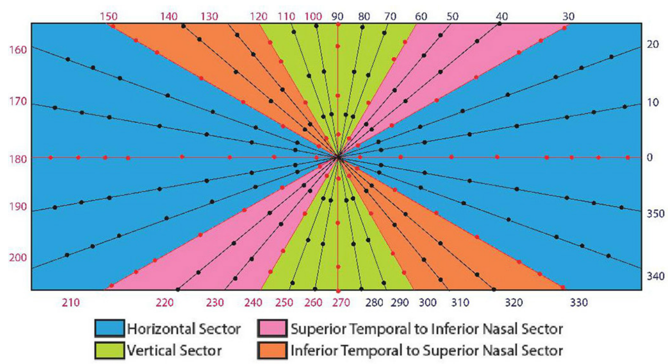

Sector-wise representation of the 185 predetermined locations (black and red dots) where refraction was measured.
Commercial Relationships: Keyur Savla, None; **Viswanathan Ramasubramanian**, None

Program Number: 1134 **Poster Board Number:** B0554
Presentation Time: 3:15 PM–5:00 PM
Effect of marginally induced astigmatism on refractive error development in chicks
Sowmya Ravikumar, Elysia M. Ison, Christine F. Wildsoet. University of California Berkeley, Fremont, CA.
Purpose: We investigated the effect of marginally induced astigmatism on refractive error development and eye growth in chicks.
Methods: Four groups of chicks were fitted with custom-made two-zone spectacle lenses on one eye, the other serving as control, one week after hatching. Lenses for two treatment groups were Plano in the center and +15D cylinder at axis 90 in the periphery. The other two groups wore lenses that were Plano in the center and +15D sphere in the periphery. One sphere group and one cylinder

group were fitted with lenses that had 5.5mm central zone diameter (CZD) and the other sphere and cylinder group, with 4.5mm CZD. Each group had 10 chicks. The White-Leghorn chicks were raised with normal diurnal lighting (12 hours off/on). All animal care and treatments conformed to the ARVO statement for the Use of Animals in Ophthalmic and Vision Research. Retinoscopy and A-scan ultrasound were performed before, 3, 6 &9 days after lens insertion. Refraction, Axial length and other biometric parameters were compared across the groups.
Results: At 9 days of treatment, mean inter-ocular difference (IOD = Treatment eye – Control eye) in spherical equivalent refractive error was -7.53+/-1.81D, for the +15DS periphery 5.5mm CZD; -3.78+/-0.91D, for the +15DCX90 periphery 5.5mm CZD; -11.5+/-1.95D for the +15DS periphery 4.5mm CZD and -4.15+/-2.68D for the +15DCX90 periphery 4.5mm CZD. Optical axial length of treated eyes was shorter than control eyes in both spherical periphery groups (mean IOD of -0.371mm). The Vitreous Chamber Depths of treated eyes were shorter than the control eyes (mean IOD of -0.24mm), with the differences increasing with duration of lens wear. No statistically significant change was observed either in axial length or vitreous chamber depth for either of the cylindrical groups. Statistically significant choroidal thickening was observed in all four groups, although, the change was larger in the spherical group compared to cylindrical group.
Conclusions: Whereas with induced spherical defocus, the changes in refraction continue to happen monotonically over the course of treatment, with induced cylindrical defocus there is an initial shift to hyperopic refraction, followed by a plateau. Nonetheless, when marginal light rays are astigmatically defocused, refractive development is biased towards the plane of best paraxial focus, not the most myopic plane of best focus for one meridian.
Commercial Relationships: Sowmya Ravikumar; **Elysia M. Ison**, Cooper Vision (F); **Christine F. Wildsoet**, Cooper Vision (F)
Support: 1K08EY025010-01A1 to SR and 5R01EY012392-15 to CFW

Program Number: 1135 **Poster Board Number:** B0555
Presentation Time: 3:15 PM–5:00 PM
Pilot testing of a miniature autorefractor
Ying-Ling Chen[1], Lei Shi[2], J W L. Lewis[2]. [1]Center for Laser Applications, University of Tennessee Space Institute, Tullahoma, TN; [2]E-Vision Technologies Inc., Tullahoma, TN.
Purpose: To develop and test a cost-effective, palm-size autorefractor.
Methods: The presented infrared autorefractor employs the eccentric photorefraction (EPR) technique and a Badal optometer system similar to what was proposed by Roorda in 1998 [1]. The refractive state of the eye is measured by moving the EPR camera behind the Badal lens until the crescent shape of pupil light distribution reverse to opposite side like the retinoscopy. The reversing of light corresponds to the situation when the EPR camera is conjugate to the eye's retina. Several modifications were made to the system. To reduce the system size, a miniature camera with an entrance pupil less than 1.5 mm was used together with fiber optics that provided accurate positioning of illumination. The Badal optometer used a 25 diopter lens to extend the measurement capability. A 0.5-second full-range pre-scan estimated the region of spherical equivalent and determined the subsequent fine scanning region for astigmatic assessment. The resolution of scanning step-motor was 0.08 diopter. We tested the functional prototype on our own eyes with contact lenses and with an artificial eye with adjustable pupil size from 3.3 to 8.8 mm and refractive error from -7 diopters to +6 diopter.
[1] A. Roorda, W. R. Bobier, M. C. W. Cambell, Vis. Res. 38, 1934 (1998)
Results: Using the artificial eye with pupil size between 3.3 to 8.8 mm and refractive error between +6 and -7 diopter, the testing result showed an overall accuracy of 0.135 diopter (standard deviation). Our testing on non-cyclopleged human eyes showed repeatability with variation less than 0.25 diopter. The human images also revealed some considerations including mono-chromatic and chromatic aberrations and correlation with pupil size that require further investigation.
Conclusions: The EPR optometer presents a technique that is easy to perform without need of careful alignment or calibration for individual or environment differences. This pilot study showed that it is capable to rapidly determine refraction in extended range with decent accuracy.
Commercial Relationships: Ying-Ling Chen, University of Tennessee Research Foundation (P); **Lei Shi**, E-Vision Technologies Inc. (E); **J W L. Lewis**, E-Vision Technologies Inc. (P)

Program Number: 1136 **Poster Board Number:** B0556
Presentation Time: 3:15 PM–5:00 PM
A machine learning approach to determine refractive errors of the eye
Arne Ohlendorf[1, 2], Alexander Leube[2], Christian Leibig[2], Siegfried Wahl[1, 2]. [1]Technology and Innovation, Carl Zeiss Vision International GmbH, Aalen, Germany; [2]Insitute for Ophthalmic Research, Eberhard Karls University Tuebingen, Tuebingen, Germany.
Purpose: In order to account for the neural contributions to perception, refractive errors of the eye are traditionally assessed by a subjective measurement, or by using mechanistic models, like image quality metrics. The aim of this research was to explore the suitability of a machine learning approach to identify the perceptually optimal sphero-cylindrical refraction correction, when compared to subjective measurements.
Methods: The data of 460 eyes from 230 subjects with a mean age of 33.1 ± 11.5 years (range: 18 to 78 years) were included in the study. The subjective assessment of the non-cycloplegic refractive errors under monocular conditions were performed by two optometrists using a digital phoropter (ZEISS Visuphor 500, Carl Zeiss Vision GmbH, Germany) and SLOAN optotypes. Wavefront aberrations were approximated by Zernike polynomials up to the 7th radial order (i.Profiler plus, Carl Zeiss Vision). A multilayer perceptron (MLP) with two hidden layers was trained to predict the sphero-cylindrical refraction correction from 37 dimensional feature vectors (36 Zernike coefficients + pupil diameter). All data was used for training and testing purposes via 10-fold cross validation. Bland Altman analysis was performed to investigate the mean differences and the 95% Limits of Agreement (LoA) between refractive components (M, J_0 and J_{45}) from MLP predictions and independent subjective refractions.
Results: Using the machine learning approach to predict the power vectors of refraction, the mean squared error (MSE) of the prediction (M: MSE = 0.17 D^2; J_0 MSE = 0.03 D^2; J_{45} MSE = 0.03 D^2) resided in a similar range as the resolution commonly used for subjective prescriptions (M: 0.14 D^2; J_0 and J_{45}: 0.02 D^2). 95% of the predictions were contained in the interval of ±0.83 D (M), ±0.35 D (J_0) and ±0.34 D (J_{45}) respectively. These intervals are comparable to those previously observed for both mechanistic models and subjective assessments of refraction. The bias with respect to subjective measurements is trivially close to zero for all three vector components (ΔM = 0.00 D, ΔJ_0 = 0.01 D and ΔJ_{45} = 0.02 D).

Conclusions: The neural network based prediction of the refractive correction lead to comparable values of the power vectors of refraction, when compared to the subjective measurements.
Commercial Relationships: Arne Ohlendorf; **Alexander Leube**, None; **Christian Leibig**, None; **Siegfried Wahl**, Carl Zeiss Vision International GmbH (F)

Program Number: 1137 **Poster Board Number:** B0557
Presentation Time: 3:15 PM–5:00 PM
Wavefront-based autorefraction on a telemedicine platform
Kaccie Y. Li, Huy Tran, David Shu. Smart Vision Labs, New York, NY.
Purpose: SVOne Enterprise by Smart Vision Labs (SVL) integrates wavefront sensing on a smartphone with a proprietary telemedicine platform. Refractive-error measurements along with other clinically relevant data are collected and transmitted for an ophthalmologist to remotely review and generate a prescription (Rx). In this study, we evaluate the agreement between SVOne-produced autorefraction (AR) results and the final doctor's Rx.
Methods: Fifty-four healthy eyes, 27 individuals (ages 18 to 60), went through an SVOne Enterprise in a retail setting. Fourteen individuals provided glasses which were measured and entered into the platform (lensometer data). Image-processing algorithms built into the SVL iOS app automatically recognizes, captures and analyzes 3 Shack-Hartmann spot images to produce each AR result. Furthermore, every individual goes through a standard ocular health questionnaire and visual acuity test both of which are conducted through the app. All results along with Shack-Hartmann images and technician comments on patient satisfaction of current glasses (if available) are transmitted through SVL's HIPAA-compliant platform to a panel of ophthalmologists for review. An ophthalmologist-prescribed R_x is emailed within 24 hours.
Results: Final R_x ranged from -8.00 D to 3.00 D and -1.50 D to 0.00 D for SPH and CYL respectively. Across the board results for AR and R_x differed on average by 0.40 D. Agreement improves to 0.23 D when lensometer data was not available to the ophthalmologists. Comparison of cylindrical correction (CYL and AXIS) for the lensometer group was not made due to doctors often prescribing directly off the lensometer. When lensometer data is not available, CYL differed by an average of 0.35 D while R_x AXIS was generally taken directly from AR. No CYL was prescribed for 3 eyes with AR-measured CYL of -0.25 D; it was also ignored for 2 eyes with greater levels of CYL (-0.75 D and -1.00 D).
Conclusions: A telemedicine platform built on wavefront-sensing technology was developed for providing eyeglass prescriptions in a retail setting. Agreement between AR and R_x for SPH is excellent. Prescribing habits using lensometer data for cylindrical correction varied greatly across different ophthalmologists not allowing for a meaningful comparison between AR and R_x. However when lensometer data was not available, agreement between AR and R_x for CYL and AXIS is good.

Commercial Relationships: Kaccie Y. Li, Smart Vision Labs (E); **Huy Tran**, Smart Vision Labs (E); **David Shu**, Smart Vision Labs (E)

Program Number: 1138 **Poster Board Number:** B0558
Presentation Time: 3:15 PM–5:00 PM
Fast automated subjective refraction
Jaume Pujol[1], Carles Otero[1], Mikel Aldaba[2], Fernando Díaz-Doutón[1, 2]. [1]Davalor Research Center (dRC). Universitat Politècnica de Catalunya, Terrassa, Spain; [2]Centre for Sensors, Instruments and Systems Development (CD6), Universitat Politècnica de Catalunya, Terrassa, Spain.
Purpose: To investigate a new method to perform a fast non-cycloplegic refraction that includes the patient's psychophysical response without clinician support.
Methods: Seventy-five healthy subjects were measured twice with the FASR (test-retest) and once with the conventional clinical refraction procedure (CSR). FASR procedure started from the objective refraction (sph, cyl, ax) obtained with an autorefractometer and computed all possible refractions in the interval [(sph-0.50, cyl, ax):(sph+1.50, cyl+1, ax)] in steps of 0.25 D for cylinder and sphere. All the generated refractions were transformed to power vectors and the Euclidean distances with respect the objective refraction were sorted. Then, the root finding bisection algorithm was applied to the Euclidean distances. The algorithm was implemented on a stereoscopic virtual reality system capable of changing sphero-cylindrical refractions according to patient's responses that also has an embedded autorefractometer (Eye and Vision Analyzer, EVA, Davalor Salud Spain). Main outcome measure: spherical equivalent (M) and Jackson cross-cylinder (J_0 and J_{45})
Results: The new proposed method took 4 minutes and 12 seconds (± 99 seconds) and the conventional standard procedure took 12 minutes and 5 seconds (± 316 seconds). The time difference was statistically significant (paired sample t-test, $p<0.01$, $t=-19.71$). The within-subject standard deviations between test-retest (i.e., repeatability) of the new method for the right eye were 0.30, 0.12 and 0.06 D for M, J_0 and $J_{45,}$ respectively. The mean power vector (M, J_0 and J_{45}) differences (±SD) for the right eye between the new method and the conventional procedure were, respectively, 0.08 (±0.36), -0.02 (±0.17) and -0.03 D (±0.09).
Conclusions: The repeatability of the new method and the agreement with conventional subjective refraction are similar to the repeatability and reproducibility of the conventional subjective refraction reported in other studies. While this method presents some limitations that warrant further investigation (e.g., neural response to virtual reality displays), the results of this study show a potential fast, new method of performing subjective refraction without clinician support in a healthy population.
Commercial Relationships: Jaume Pujol, DAVALOR SALUD S.L (P), DAVALOR SALUD S.L (F); **Carles Otero**, DAVALOR SALUD S.L (P), DAVALOR SALUD S.L (F); **Mikel Aldaba**, None; **Fernando Díaz-Doutón**, DAVALOR SALUD S.L (F)
Support: Spanish Ministry of Economy and Competitiveness grant DPI2014-56850-R ; Davalor Salud, S.L (Spain); Generalitat de Catalunya by Predoctoral grant FI-DGR (CO)

Program Number: 1139 **Poster Board Number:** B0559
Presentation Time: 3:15 PM–5:00 PM
Clinical validation of a novel wavefront autorefractor in a base hospital and vision center in rural India
Nicholas J. Durr[1, 2], Shivang R. Dave[2], Daryl Lim[2], Ramakrishnan Mahadevan[4], Sriram Ravilla[4], Sanil Joseph[3], Thulasiraj D. Ravilla[3, 4], Eduardo Lage[2, 5]. [1]Department of Biomedical Engineering, Johns Hopkins University, Baltimore, MD; [2]PlenOptika, Inc., Boston, MA; [3]Aravind Eye Care System, Madurai, India; [4]Aurolab, Madurai, India; [5]Department of Biochemistry, Universidad Autonoma de Madrid, Medical School, Madrid, Spain.

Purpose: To assess the best-corrected visual acuity (VA) and patient preference for eyeglasses prescribed by a novel autorefractor and an experienced refractionist in south India.
Methods: Participants were recruited from patients scheduled for a general refraction at Aravind Eye Hospital (base hospital, N=506; and satellite vision center, N=202). Patients were prescribed eyeglasses via subjective refraction (L_{SR}) by an ophthalmic technician with over four years of refraction experience. Consenting patients that were within the range of the autorefractor (-6D to +10D) were enrolled in the study. Participants were then prescribed eyeglasses with an autorefractor (L_{AR}) that was an alpha prototype of the QuickSee wavefront aberrometer. The QuickSee is handheld, binocular, open-view, intended to be low-cost, and was operated by a technician with no formal eye care training. The VA and prescription preferences for trial lenses set to L_{SR} and L_{AR} were evaluated by a refractionist blinded to the prescription source. The right-eye VA for each patient was converted to LogMar values and analyzed with a paired t-test. Prescription preferences were determined with a survey.
Results: The mean age of participants was 35 ± 13 years (range: 15-70). Of the 708 participants, 220 had presbyopia, 75 had an immature cataract, 21 had conjunctivitis, and 1 had keratoconus. Mean VA was 0.29 ± 0.36, -0.04 ± 0.11, and -0.01 ± -0.15 LogMar units before correction, with L_{SR}, and with L_{AR}, respectively. VA was significantly better after correction from both prescription methods ($p < 0.01$). VA from L_{SR} was also significantly better than L_{AR} ($p < 0.01$). A total of 47%, 91%, and 85% of patients had 20/20 vision or better, before correction, with L_{SR}, and with L_{AR}, respectively. Survey results showed 25% of participants had no preference of eyeglasses, 42% preferred L_{SR}, and 33% preferred L_{AR}.
Conclusions: Our study shows a small benefit to eyeglasses prescribed by subjective refraction versus a novel autorefractor. Participants using eyeglasses prescribed by the autorefractor achieved a VA that was only approximately one letter worse than using eyeglasses prescribed by a refractionist. More than half of the participants either had no preference or preferred eyeglasses prescribed by the autorefractor. However, the required training to perform autorefraction is considerably shorter compared to subjective refraction.
Commercial Relationships: Nicholas J. Durr, MIT (P), PlenOptika (I); **Shivang R. Dave**, MIT (P), PlenOptika (I), PlenOptika (E); **Daryl Lim**, MIT (P), PlenOptika (I), PlenOptika (E); **Ramakrishnan Mahadevan**, Aurolab (E); **Sriram Ravilla**, Aurolab (E); **Sanil Joseph**, None; **Thulasiraj D. Ravilla**, Aurolab (E); **Eduardo Lage**, MIT (P), PlenOptika (E), PlenOptika (I)

Program Number: 1140 **Poster Board Number:** B0560
Presentation Time: 3:15 PM–5:00 PM
Spurious image methodology: from optical bench to clinical assessment
Henk A. Weeber, Marrie Van der Mooren, Selma Boersma, Aixa Alarcon, Patricia A. Piers. R & D, AMO Groningen BV, Groningen, Netherlands.
Purpose: Pseudophakic patients implanted with presbyopia correcting (PC) lenses may experience photic phenomena originating from spurious images. Specific spurious images that occur are the halo(s) originating from bifocal or trifocal lenses, which may be bothersome for patients. Photometric evaluation of halos can be evaluated pre-clinically. However, the challenge remains to translate pre-clinical evaluation to the potential bothering effect that may be experienced by patients.
Methods: Methodology has been presented in the past for measuring the size and light intensity of halos (van der Mooren, ARVO 2016). In this study we evaluated the robustness of this method. Specifically, we evaluated the reproducibility and the potential of the method to distinguish between halo performance of different lens designs. Measurement data of a monofocal IOL and a multifocal IOL were collected retrospectively. The measurement data were processed in order to obtain the relative light intensity (RLI) as a function of visual angle. RLI was expressed in a logarithmic scale. Reproducibility was calculated, and the difference between halo of the monofocal IOL and a multifocal IOL was evaluated using a student-t test.
Results: Ten monofocal IOLs and 9 multifocal IOLs were measured on different days over a time period of 5 years (2010 to 2015). Within a visual angle of 1 degree, the dynamic range for the monofocal IOL was 10 times larger as compared to the multifocal IOL (monofocal IOL: 4.18 decades, multifocal IOL: 3.30 decades). The reproducibility of the monofocal IOL and the multifocal IOL were not significantly different (P=0.36). The pooled reproducibility standard deviation is 0.17 decades.
The difference in RLI between the two IOL models varied from 0 to 1.3 decades. The difference was statistically significant for visual angles of 0.1 degree and larger. Results indicate that more subtle differences between lens designs can also be measured. Comparison with literature data indicates that the reproducibility is considerably better than the variance in clinically measured halos (Pieh et al. 2001), while also the clinically measured halos noticed a clear distinction between multifocal and monofocal halo.
Conclusions: The in-vitro halo measurement method described is capable of providing halo intensity profiles. The reproducibility seems adequate for measuring small differences between lens designs.
Commercial Relationships: Henk A. Weeber, Abbott Medical Optics (E); **Marrie Van der Mooren**, Abbott Medical Optics (E); **Selma Boersma**, Abbott Medical Optics (E); **Aixa Alarcon**, Abbott Medical Optics (E); **Patricia A. Piers**, Abbott Medical Optics (E)

Program Number: 1141 **Poster Board Number:** B0561
Presentation Time: 3:15 PM–5:00 PM
A Method to Measure Objective Refraction in Small-Aperture Corneal Inlay Patients
Colin E. Brown[1], Mollie Myers[2], Lance Kugler[2], Srividhya Vilupuru[3]. [1]Ophthalmology, University of Nebraska Medical Center, Omaha, NE; [2]Kugler Vision, Omaha, NE; [3]AcuFocus, Inc., Irvine, CA.
Purpose: Small-aperture corneal inlay (KAMRA, AcuFocus Inc., Irvine CA) improves near vision in presbyopic patients by extending depth of focus in the inlay eye. At present, it can be difficult for autorefractors to reliably measure objective refraction in eyes implanted with a small-aperture inlay. The AcuTarget HD (ATHD, Visiometrics, Spain), a new diagnostic instrument based on the double-pass technique, measures objective spherical equivalent refraction (SE). The purpose of this study was to determine whether the objective SE measured by ATHD is consistent with the subjective manifest refractive spherical equivalent (MRSE) in eyes implanted with the small-aperture corneal inlay.
Methods: In a retrospective study, twelve patients implanted monocularly with a small-aperture corneal inlay were examined at 1, 3 and 6 months postoperatively. A comprehensive eye examination, including uncorrected and best-corrected visual acuities, manifest spherocylinder refraction, ATHD objective refraction and slit lamp examination, was performed at each visit. Refractions were performed by a single refractionist (MM). The subjective MRSE was calculated from the measured manifest spherocylinder refraction. Mean ± Standard deviation (SD) of objective SE, subjective MRSE and correlation between the refractions were determined by analyzing pooled data across all three visits (n = 36) and at each individual visit (n = 12).

Results: For data pooled across visits, the mean ± SD of objective SE and subjective MRSE were -0.27 D ± 0.67 D and -0.44 D ± 0.78 D, respectively. The objective SE was within ± 0.50 D of subjective MRSE in 69.4% and within ± 1.0 D in 91.7% of measurements. Linear regression analysis between objective SE and subjective MRSE showed a statistically significant relationship ($R^2 = 0.50$, $F(1, 35) = 33.61$, $p < 0.0001$). Similarly, the two refraction measurements were significantly correlated at month 1 ($R^2 = 0.66$, $F(1, 11) = 19.41$, $p = 0.0013$) and month 6 ($R^2 = 0.74$, $F(1, 11) = 25.04$, $p = 0.0007$). The two refraction measures showed a weak correlation at month 3 ($R^2 = 0.19$, $F(1, 11) = 2.58$, $p = 0.1365$).
Conclusions: The objective refraction measurement from ATHD was found to be similar to the subjective manifest refractive spherical equivalent. The ATHD instrument can be used to estimate the subjective refraction in the patients implanted with the small-aperture inlay.
Commercial Relationships: Colin E. Brown, None; **Mollie Myers**, None; **Lance Kugler**, Abbott Medical Optics (C), Alphaeon (I), Strathspey Crown (I); **Srividhya Vilupuru**, AcuFocus (E)